International Journal of Physical Sciences Vol. 2(2), pp. 021-031, February 2014
Available online at http://academeresearchjournals.org/journal/ijps
ISSN 2331-1827 ©2014 Academe Research Journals

Full Length Research Paper

Isolated condition detection based on voltage analysis for renewable energy

Mehdi Noushyar * and Behrouz Sobhany

Technical Engineering Department, University of Mohaghegh Ardabili, Ardabil, Iran.

Accepted 24 February, 2014

The increasing electrical power demand has caused Distributed Generations (DGs) to enter into the power systems which created many problems in power systems. One of these problems is unwanted islanding phenomenon. Personnel and equipment safety are the main reasons concerning which this condition should be detected in the fastest possible time. A novel passive islanding detection algorithm based on histogram analysis for wind turbines is presented in this paper. The proposed method measured the voltage signal of wind turbine and detected islanding condition based on its sum square error. The sampling window was selected from system time constant in islanding mode for reliable and fast detection. One of the big disadvantages of passive detection methods is threshold value of these methods. In order to overcome this drawback, the threshold value in this study was determined using thresholding algorithm. The presented studies are based on time-domain simulations using MATLAB. The results' evaluation confirms that the proposed islanding detection method succeeds in detecting islanding mode from other switching conditions.

Key words: Islanding detection, wind turbine, passive method, distributed generation.

INTRODUCTION

Distributed Generations (DGs) generally refer to Distributed Energy Resources (DERs), including photovoltaic, fuel cells, micro turbines, small wind turbines, and additional equipment. In recent years, the increase of distributed resources in the electric utility systems with ongoing technological, social, economical and environmental aspects shows high depth of penetration of DGs. With improvement in DGs technologies and power electronics, DG units have become more competitive against the conventional centralized system. Hence, it attracts many customers from industrial, commercial, and residential sectors (Zeineldin et al., 2006a; Wen-Jung et al., 2012; Jiayi et al., 2008).

Many utilities around the world already have significant penetration of DGs in their system. Annually, the total global installed wind capacity at the end of 2010 was 2.5% of the total global demand. Based on the current growth rates, World Wide Energy Association (WWEA) predicts that in the end of the year 2020, at least 1500 GW can be expected to be installed globally (http://www.renewableenergyworld.com/rea/news/article/2011/05/worldwind-outlook-down-but-not-out). When the distributed generation systems are operated in parallel with utility power systems, especially with reverse power flow, the power quality problems become significant. Power quality problems include frequency deviation, voltage fluctuation, harmonics and reliability of the power system. In addition, one of the technical issues created by DG interconnection is inadvertent islanding (Dash et al., 2012; Zeineldin et al., 2006b). Islanding occurs when a DG and its local load become electrically isolated from the utility; meanwhile, the DG produces electrical energy and supplies the local load (Jayaweera et al., 2007). Islanding condition causes abnormal operation in the power system and also causes negative impacts on protection, operation, and management of distribution systems. Therefore, it is necessary to effectively detect the islanding conditions and swiftly disconnect DG from the network. Existing standard thus do not permit DGs to be utilized in islanding mode (Zeineldin et al., 2007) because islanding creates many problems (Xu et al., 2004; Swisher et al., 2001) in power systems such as: safety hazards for personnel, power quality problems for customers load, overload conditions of DG, out-of-phase recloser connections. In order to avoid the above

*Corresponding author. E-mail: mnooshyar@yahoo.com.

problems occurring, islanding conditions should be detected within less than 2 s (Xu et al., 2004).

Originally, the methods of islanding detection were divided into two categories: communication and local. Local methods were classified as active and passive techniques, in which active techniques are based on direct interaction with the ongoing power system operation (Zeineldin et al., 2007). Some important active techniques are impedance measurement, frequency shift and active frequency drift (Chowdhury et al., 2009), current injection (Hernández-González and Iravani, 2006), Sandia frequency shift and Sandia voltage shift (John et al., 2004), and negative phase sequence current injection (Karimi et al., 2008). Active methods are usually used in converter based distributed generator. Passive techniques that are used in induction wind turbine generator are based on measurements and information at the local site. Over/under voltage and frequency is one of the simplest passive methods used in islanding detection. Unfortunately, if the load and the generation on the island are closely matched, the change in voltage and frequency might be very small and within the thresholds, thus leading to an undetected islanding situation. Other passive techniques have been proposed based on monitoring rate of change of frequency (ROCOF) (El-Arroudi et al., 2007) and rate of change of phase angle drift (ROCOPAD), phase angle displacement, rate of change of generator power output (Chowdhury et al., 2009), impedance monitoring, the THD technique (http://www.renewableenergyworld.com/rea/news/article/ 2011/05/worldwind-outlook-down-but-not-out) non detection zone concept (Zhihong et al., 2004), vector surge and phase displacement monitoring (Kunte and Gao, 2008) and the wavelet transform function (Cheng-Tao et al., 2008).

A novel technique for islanding detection based on voltage histogram signal is proposed in this paper. The proposed approach used the Mean Absolute Error (MAE) of voltage histogram signal, which in the islanding mode is higher than the grid connected mode. The results in several conditions of local loads can prove this pretense and illustrate its robust performance for islanding detection. Also, negligible NDZ is one of the many advantages of the proposed method. This approach measures the voltage signal at the target distributed generation location and feeds it to the proposed histogram based algorithm in order to detect the islanding condition from other conditions.

The proposed technique, which is suitable for asynchronous DGs, is explained as the study proceeds. This is followed by an explanation of the simulation and experimental test system used to verify the effectiveness of the proposed method. Afterwards, the effectiveness and robustness of the proposed algorithm applied to the simulation and experimental test systems is explored in comparison with the recently reported method in (Kazemi and Sobhani, 2012), after which the paper is concluded. The simulation test systems were simulated in MATLAB/SIMULINK. The simulation and experimental results show that the proposed islanding detection technique can successfully detect islanding operations within acceptable time duration.

CASE STUDY

The study test system is shown in Figure 1. The DG unit is a wind turbine induction generator whose rated voltage is 0.69 kV and is connected to a Point of Common Coupling (PCC) with a step-up transformer whose rated power is 1.5 MVA. The local load is a three-phase parallel RL before the circuit breaker (CB), in which “*r*” stands for the series resistance inductance and R_L is the parallel load that is connected to the system in Y connection. In order to correct the power factor, a capacitor bank was used. Local load and system parameters are given in Table 1. In the grid-connected condition, the islanding mode occurs when SW2 is open. For the evaluation of islanding detection techniques, the parallel R_L is traditionally adopted as the local load when the load inductance is adjusted to the system frequency. The amount of local load and capacitor should be set to allowable amount, that in islanding condition the voltage, current and frequency remain in allowable value.

It should be noted that the frequency and voltage of DG should have admissible values in both grid-connected and islanded modes. In the grid-connected condition, the voltage magnitude and frequency of the local load at the PCC are regulated by the grid.

MATHEMATICAL MODEL OF ISLANDED SYSTEM

State-space mathematical model for the islanded system was provided in this study. In the islanding mode, the circuit model of wind turbine with fixed wind speed is shown in Figure 2a and the simple model is shown in Figure 2b. It is assumed that the DG unit and the local load are balanced three-phase subsystems within the island. The state space equations of the potential island of Figure 2 in the standard state space form are:

$$\begin{aligned} \dot{X}(t) &= AX(t) + Bu(t) \\ y(t) &= CX(t) \\ u(t) &= v_{td} \end{aligned} \tag{1}$$

In the balanced three-phase subsystems within the island, the state-space model is:

$$\begin{cases} v_g^{abc}(t) = L_s \dfrac{di_g^{abc}(t)}{dt} + r_s i_g^{abc}(t) + v_t^{abc}(t) \\ i_g^{abc}(t) = i_m^{abc}(t) + C\dfrac{dv_t^{abc}(t)}{dt} + \dfrac{1}{R_L} v_t^{abc}(t) \\ v_t^{abc}(t) = L_m \dfrac{di_m^{abc}(t)}{dt} + r_m i_m^{abc}(t) \end{cases} \tag{2}$$

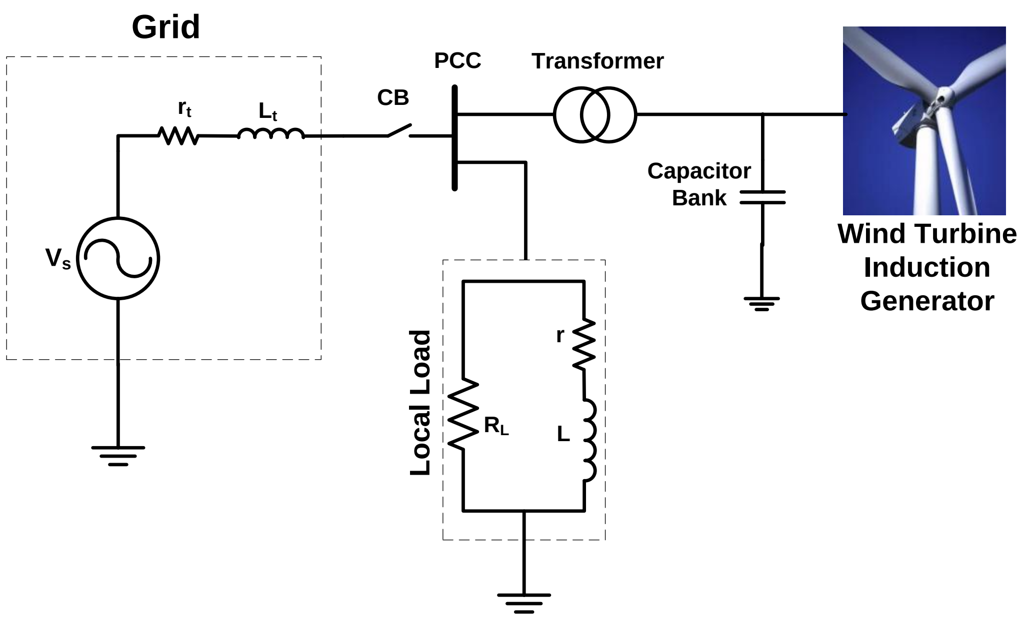

Figure 1. Single line diagram of the study system.

Table 1. Local load and system parameters.

DG nominal power	660 KVA
Voltage$_{rms}$ (L-L)	0.69 kV
r_s	0.5269 Ω
L_s	17.1 mH
Nominal frequency	50 HZ
R	2667 Ω
L	2.37 H
C	1.592 μF

In the $\alpha\beta$ -frame, the dynamic model of the system is:

$$\begin{cases} v_g^{\alpha\beta}(t) = L_s \dfrac{di_g^{\alpha\beta}(t)}{dt} + r_s i_g^{\alpha\beta}(t) + v_t^{\alpha\beta}(t) \\ i_g^{\alpha\beta}(t) = i_m^{\alpha\beta}(t) + C\dfrac{dv_t^{\alpha\beta}(t)}{dt} + \dfrac{1}{R_L} v_t^{\alpha\beta}(t) \\ v_t^{\alpha\beta}(t) = L_m \dfrac{di_m^{\alpha\beta}(t)}{dt} + r_m i_m^{\alpha\beta}(t) \end{cases} \quad (3)$$

With transfer to rotating reference frame ($x_{\alpha\beta} = x_{dq}e^{j\theta}$) and assuming of constant frequency in islanded condition and V_t as reference frame:

$$\begin{cases} \dfrac{di_{gd}(t)}{dt} = \dfrac{1}{L_s} v_{gd}(t) - \dfrac{r_s}{L_s} i_{gd}(t) + \omega i_{gq}(t) - \dfrac{1}{L_s} v_{td}(t) \\ \dfrac{di_{gq}(t)}{dt} = -\omega i_{gd}(t) - \omega i_{gd}(t) + \dfrac{1}{L_s} v_{tq}(t) \\ \dfrac{dv_{td}(t)}{dt} = \dfrac{1}{C} i_{gd}(t) - \dfrac{1}{C} i_{md}(t) - \dfrac{1}{CR_L} v_{td}(t) \\ \dfrac{di_{md}(t)}{dt} = \dfrac{1}{L_m} v_{td}(t) + \omega i_{mq}(t) - \dfrac{r_m}{L_m} i_{md}(t) \\ \dfrac{di_{mq}(t)}{dt} = -\omega i_{md}(t) - \dfrac{r_m}{L_m} i_{mq}(t) \\ \omega C v_{td} = i_{gd} - i_{mq} \end{cases} \quad (4)$$

Finally, the state-space equation can be written as follow:

$$\begin{bmatrix} \dot{i}_{gd} \\ i_{gq} \\ i_{md} \\ v_{td} \end{bmatrix} = \begin{bmatrix} -\dfrac{r_s}{L_s} & \omega_0 & 0 & -\dfrac{1}{L_s} \\ \omega_0 & -\dfrac{r_m}{L_m} & -2\omega_0 & \dfrac{CR_L\omega_0 r_s - L_m\omega_0}{L_m R_L} \\ 0 & \omega_0 & -\dfrac{r_m}{L_m} & \dfrac{1}{L_m} - \omega_0^2 C \\ \dfrac{1}{C} & 0 & -\dfrac{1}{C} & \dfrac{1}{CR_L} \end{bmatrix} \begin{bmatrix} i_{gd} \\ i_{gq} \\ i_{md} \\ v_{tq} \end{bmatrix} + \begin{bmatrix} \dfrac{1}{L_s} \\ 0 \\ 0 \\ 0 \end{bmatrix} \begin{bmatrix} v_{gd} \end{bmatrix} \quad (5)$$

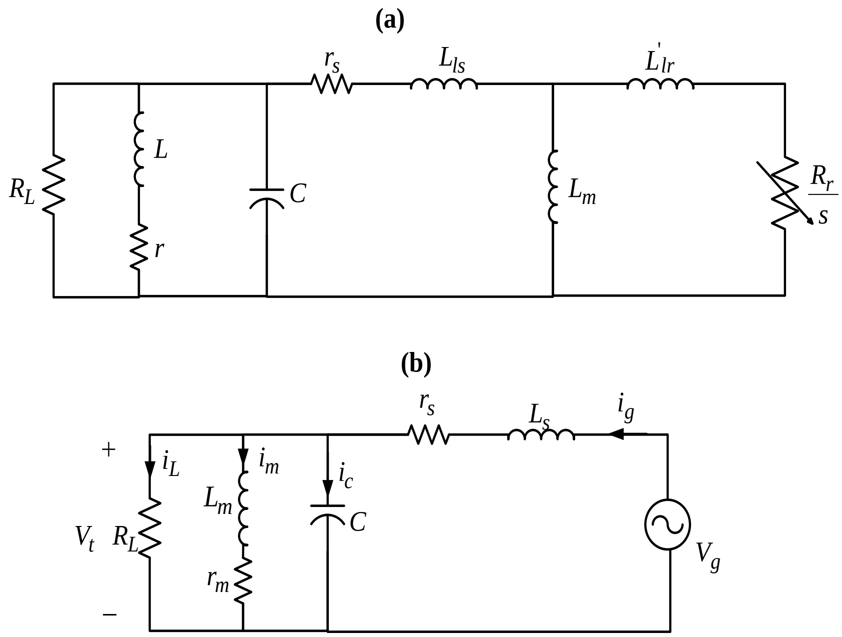

Figure 2. Model of case study: (a) original model, (b) simple model.

$$x = \begin{bmatrix} i_{gd} & i_{gq} & v_{td} & v_{tq} \end{bmatrix}^T \quad (6)$$

$$[y] = [0 \quad 0 \quad 1 \quad 0]x \quad (7)$$

$$Y(s) = C.(SI - A)^{-1}.B \quad (8)$$

$$V_d(s) = Y(s) \quad (9)$$

The transfer function of state-space model is given by:

$$V_{td}(s) = \frac{(1.5s^2 + 15.63s + 14790)e4}{(4.0e-4)s^4 + 1.359s^3 + 1.542e4s^2 + 6.266e5s + 1517e6} \quad (10)$$

The step response of output voltage is plotted in Figure 3. From Figure 3, the transient response time is about 0.15 s; we consider 0.15 s for analysis time to achieve reliable detection from step of response.

Non Detection Zone (NDZ)

In order to determine the performance of islanding detection method, Non Detection Zone (NDZ) is one of the important characteristics. NDZ is defined as an operating region where islanding conditions cannot be detected in a timely manner. In this region, power mismatch between production and consumption have a small value. Here, NDZ based on OVP/UVP and OFP/UVP was determined. This method was implemented for constant current controlled inverters. In order to determine the amount of mismatch for which the OVP/UVP and OFP/UFP will fail to detect islanding, the amount of active power mismatch in terms of load resistance can be expressed as follows:

$$\Delta P = 3 \times V \times I - 3 \times (V + \Delta V) \times I = -3 \times \Delta V \times I \quad (11)$$

where V and I show the rated voltage and current, respectively. Acceptable voltage range in distribution network is between 0.88 and 1.1 pu. These voltage levels are equivalent to $\Delta V^{pu} = -0.12$ and $\Delta V^{pu} = 0.1$, respectively. The calculated imbalance amount by Equation 11 for our test network (the output power in match condition is 150 kW), are 18 kW and -15 kW, respectively. Frequency and voltage of an RLC load has the active and reactive power as follows:

$$P_L = \frac{V_t^2}{R_L} \quad (12)$$

$$Q_L = V_t^2 \left(\frac{1}{\omega L_m} - \omega C \right) \quad (13)$$

Where, ω, P and Q are the load frequency, active and reactive power, respectively. In grid connected condition,

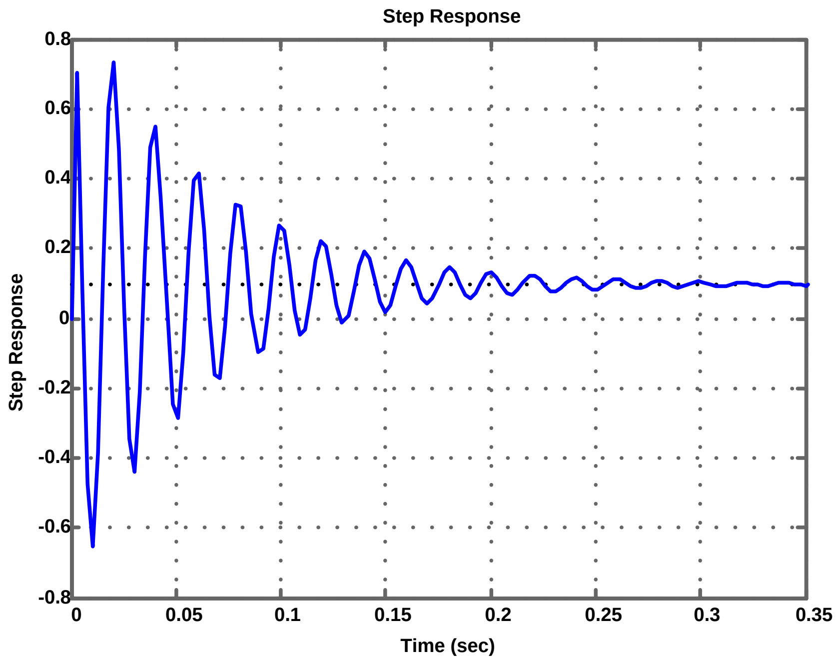

Figure 3. Step response of $V_{td}(s)$ of case study.

the voltage of PCCC is dictated by the main grid. Once the island occurred, the deviation of PCC voltage leads to active power imbalance from the nominal values. Since the output power of the inverter is in unity power factor, before islanding reactive power of load is supplied just by network and after islanding the amount of reactive power imbalance is equal to the consumed load before islanding, hence we have:

$$\Delta Q = 3\frac{V_t^2}{\omega_n L_m}\left(1-\omega^2 L_m C\right) = 3\frac{V_t^2}{\omega_n L_m}\left(1-\frac{\omega_n^2}{\omega_r^2}\right) \quad (14)$$

Where ω_n and ω_r are rated frequency and resonance frequency of load, respectively. Resonance frequency generates from imbalance power, then the frequency changes after the islanding occurrence is equal to the difference between network frequency and load resonance frequency:

$$\omega_r = \omega_n \pm \Delta\omega \;, \omega_r = \frac{1}{\sqrt{L_m C}} \quad (15)$$

Thus, the reactive power imbalance needed for certain changes in frequency can be obtained by:

$$\Delta Q = 3\frac{V_t^2}{\omega_n L_m}\left(1-\frac{f_n^2}{(f_n-\Delta f)^2}\right) \quad (16)$$

In this study, the acceptable frequency range is considered between 49.7 and 50.3 Hz which are equal to $\Delta f = -0.3$ and $\Delta f = 0.3$ Hz. Thereupon, the amounts of reactive power imbalances are 6.393 kVAr and -6.51 kVAr, respectively.

PROPOSED ALGORITHM

Let $\{0,1,2,...,M-1\}$ denote the M distinct values in a discrete signal of size N samples, and let n_i denote the number of samples with value i. The total number, N, of samples is $N = n_0 + n_1 + ... + n_{M-1}$. The normalized histogram has components (samples) $p_i = \frac{n_i}{N}$, from which it follows that:

$$\sum_{i=0}^{M-1} p_i = 1 \quad (17)$$

Inter Histogram Mean Square Error (IHMSE)

We introduce a measure for calculating the difference between two histograms and call it Inter Histogram Mean Square Error (IHMSE). Consider two histograms H1 and H2. If the total number of distinct values (M) for two histograms are the same and phji shows the ith normalized component (i=1,2 …,M) of jth (j=1,2) histogram, the IHMSE between H1 and H2 is calculated as follows:

Table 2. Various loads for islanding mode test.

Load	Case 1	Case 2	Case 3	Case 4	Case 5	Case 6
Power (kW)	146	147	148	152	154	156
R (kΩ)	2.7397	2.7211	2.7027	2.6316	2.5974	2.5641
L (mH)	3.192	3.192	3.192	3.192	3.192	3.192
C (mF)	3.174	3.174	3.174	3.174	3.174	3.174

$$IHMSE(H_1, H_2) = \frac{1}{K}\sum_{i=0}^{K-1}(n_{i1} - n_{i2})^2 \qquad (18)$$

For each possible pairs of the histograms of islanding cases, the IHMSE values are calculated and reported. Similarly for each possible pairs of the histograms of non-islanding cases, the IHMSE values are calculated and reported. These IHMSE values are called Auto IHMSE (AIHMSE) because they represent difference between two histograms which are related to the similar conditions. An IHMSE value, which is calculated between an islanding case histogram and a non-islanding case histogram, is called Cross IHMSE (CIHMSE) (Nobuyuki, 1979).

The average value of CIHMSE is greater than the average value of AIHMSE. This difference between CIHMSE and AIHMSE values motivated us to introduce an approach to classify an unknown condition, based on the calculation of IHMSE (between it and known islanding or non-islanding cases), into islanding cases or non-islanding cases.

Suppose that we have NI known islanding cases and NN known non-islanding cases. These cases are the training cases of the proposed method, then we can calculate (NI2 + NN2) and (NI×NN) possible AIHMSE and CIHMSE values respectively. All of the AIHMSE and CIHMSE values (The number of them is: NI2 + NN2+ NI×NN) are sorted out and the histogram of them is considered. This histogram is called IHMSE histogram. It is expected that the IHMSE histogram will be a bipartite histogram in which the CIHMSE values are placed in one part and the AIHMSE values are placed in another part. Thus, a proper threshold value, which is called k*, separates the IHMSE histogram into two groups.

The value of k* can be found by an appropriate thresholding method such as Otsu method (Nobuyuki, 1979). For an unknown case, if its voltage histogram is accessible, the IHMSE values between it and the known islanding cases are calculated. The average value of these IHMSEs is called k1. Similarly, the IHMSE values between it and the known non-islanding cases are calculated and the average value of these IHMSEs is called k2. By comparing the value of k* with k1 and k2, the condition of the unknown case can be determined.

SIMULATION RESULTS

Here, the test system as shown in Figure 1 is simulated by MATLAB/Simulink. The rated parameters of the system, DG, and load are listed in Table 1. The proposed islanding detection method was also tested for various conditions.

Islanding mode test

In order to show the performance of the proposed technique, the various load conditions are analyzed in islanding mode. When the imbalance of reactive power value is equal to zero and active power value is in NDZ range, the islanding detection is more difficult to identify in these conditions. The details of the test load conditions are presented in Table 2. In addition, the load quality factor is equal to 1.8 which is the maximum recommended amount in standards.

For the tested load conditions, at t=3 s, wind turbine and its local loads isolated from power grid by opening of CB and islanding mode occurred. The voltage and frequency of the PCC for each case is plotted in Figures 5 and 6, respectively. The MSE of voltage histograms between these groups is shown in Figures 7 and Table 3. It can be seen that the value of MSE between each two load conditions is variant in 0 - 19.87 range.

Switching condition

In this scenario, the load and capacitor bank switching conditions with motor starting (Figure 4) is applied to the system. These switching and starting conditions occurred at t=3 s. The voltage waveform and frequency are represented in Figures 8 and 9 respectively. MSE value of voltage histogram signals between each two switching conditions is shown in Figures 10 and Table 5.

Proposed algorithm results

Here, the mean square error between islanding conditions that are presented in Table 3, Table 5 and table 6 and non-islanding conditions that are presented in Table 4 is calculated. Table 5 shows the MSE value results. As can be seen, the value of MSE signal is different from that of the other groups. These results show the performance of the proposed method.

Conclusion

The increasing distributed generating units and enlarged size of them in a modern power system has caused the protection against islanding which has become extremely

Table 3. MSE between each two Islanding conditions (IHMSE values)

	Islanding Condition 1	Islanding Condition 2	Islanding Condition 3	Islanding Condition 4	Islanding Condition 5	Islanding Condition 6
Islanding Condition 1	0	9.16	17	15.04	11.76	18.6
Islanding Condition 2	9.16	0	8.84	9.8	14.44	11.66
Islanding Condition 3	17	8.84	0	8.96	16.62	10.58
Islanding Condition 4	15.04	9.8	8.96	0	16.28	12.82
Islanding Condition 5	11.76	14.44	16.62	16.28	0	19.78
Islanding Condition 6	18.6	11.66	10.58	12.82	19.78	0

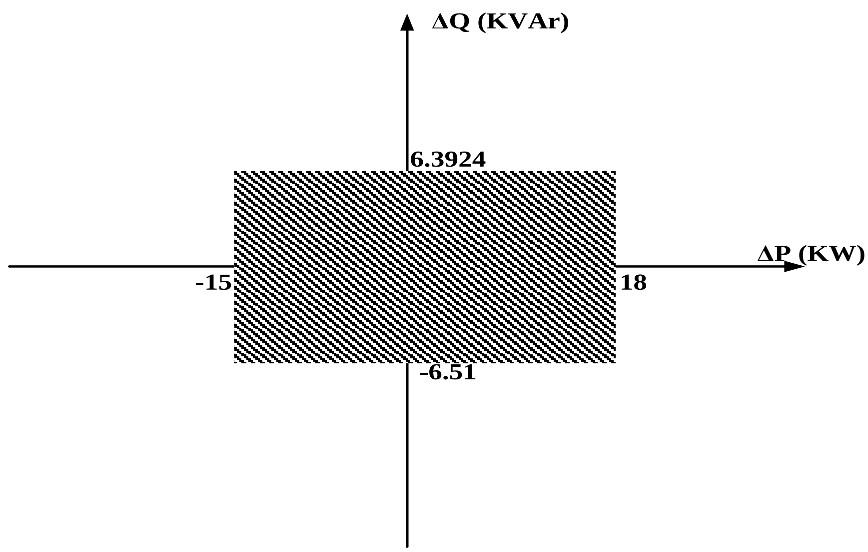

Figure 4. NDZ for the constant current interface controls for distributed generation.

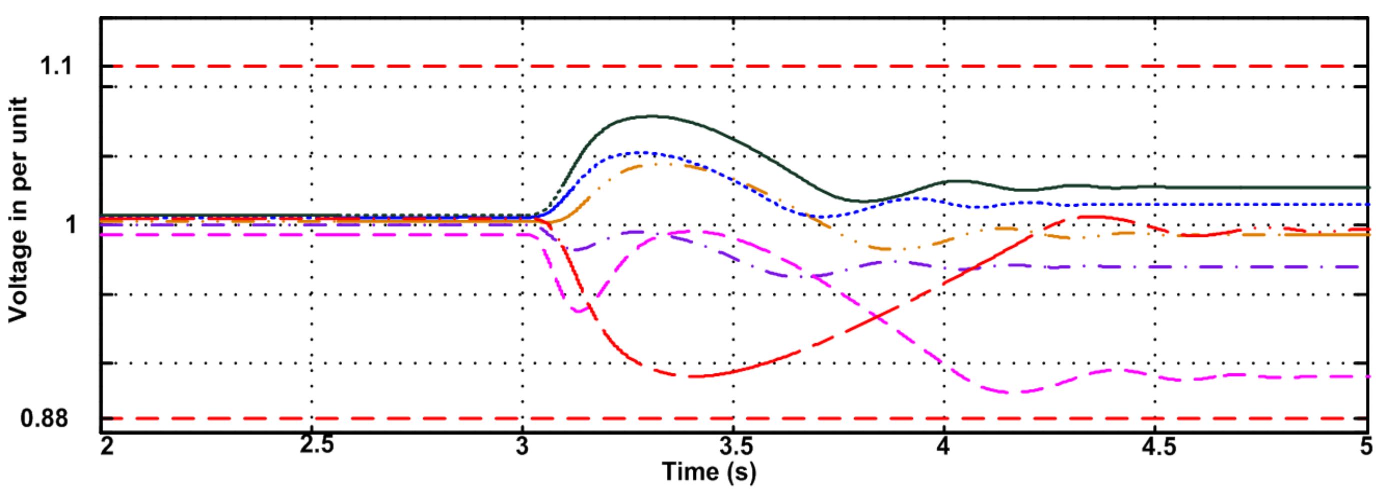

Figure 5. Effective voltage waveform of the system in islanding modes.

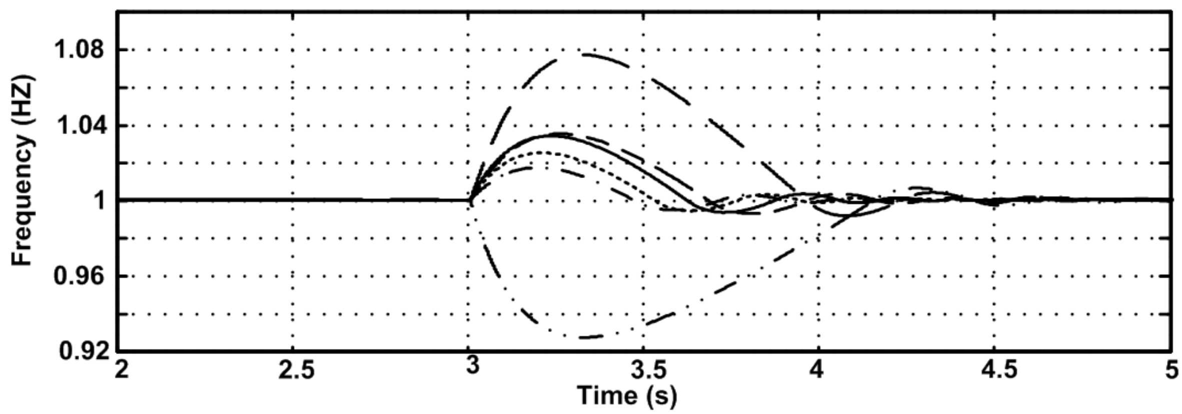

Figure 6. the frequency of system for islanding conditions.

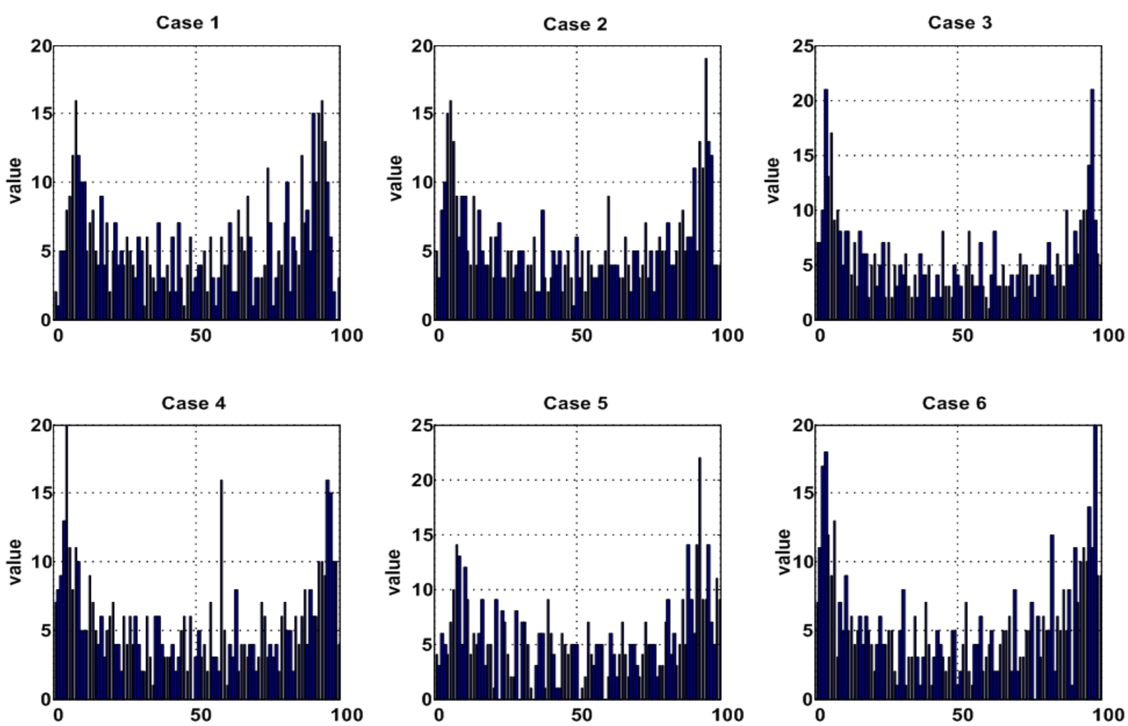

Figure 7. Histogram signal of voltage for islanding mode test.

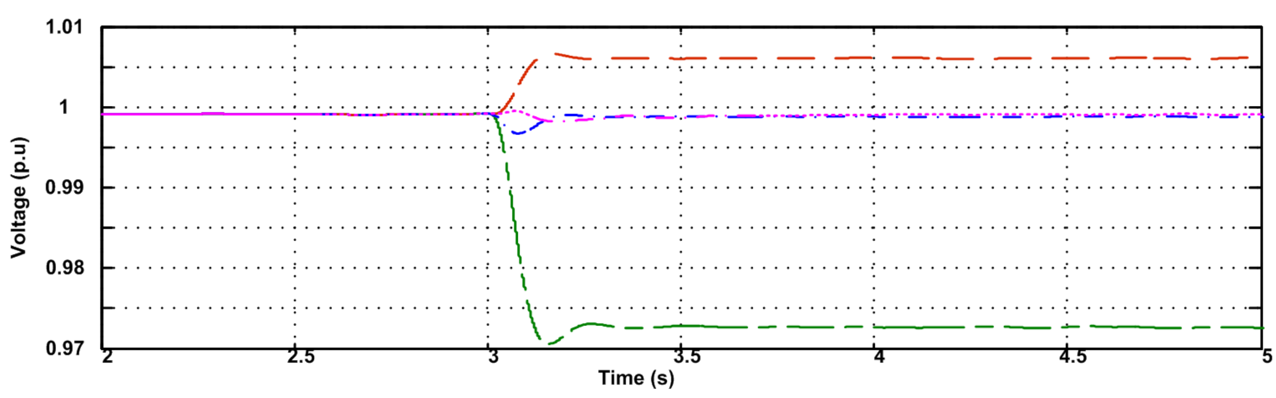

Figure 8. Effective voltage waveform of the system in switching conditions

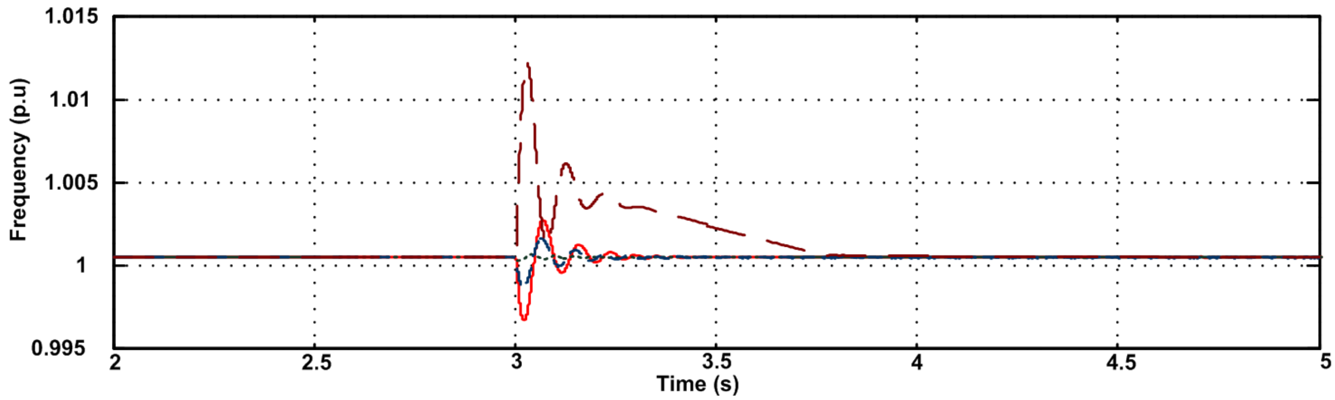

Figure 9. the frequency of system for switching conditions

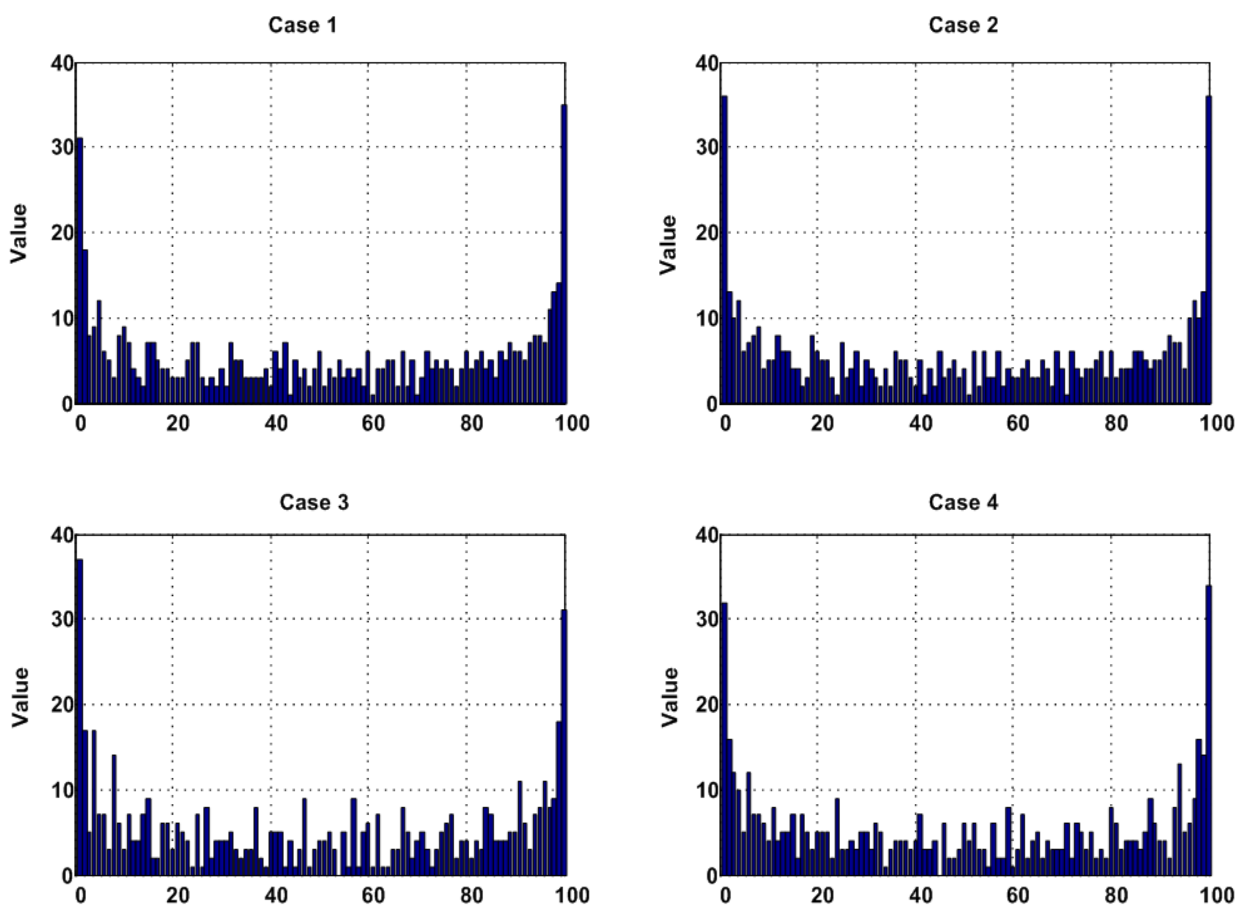

Figure 10. Histogram signal of voltage for switching mode

Table 4. Parameters of various load in switching condition

	Case 1 (Load switching)	Case 2 (Load switching)	Case 3 (Motor starting)	Case 4 (Capacitor switching)
Power (kW)	75 kW (Out)	75 kW (IN)	60 kW	
R (kΩ)	5.33	5.33	power	40 kVAr
L (H)	35.1	35.1	factor=0.78 lag	
C (μF)	0.289	0.289	(In)	

Table 5. MSE between each two switching test conditions (IHMSE values)

	Non Islanding Condition 1	Non Islanding Condition 2	Non Islanding Condition 3	Non Islanding Condition 4
Non Islanding Condition 1	0	5.88	9.96	6.06
Non Islanding Condition 2	5.88	7.60	7.60	7.56
Non Islanding Condition 3	9.96	8.84	0	10.50
Non Islanding Condition 4	6.06	7.56	10.50	0

Table 6. MSE between each two switching and islanding test conditions

	Islanding Condition 1	Islanding Condition 2	Islanding Condition 3	Islanding Condition 4	Islanding Condition 5	Islanding Condition 6
Non Islanding Condition 1	37.3	29.26	25.78	26.34	30.1	22.56
Non Islanding Condition 2	39.08	31.72	27.50	27.42	31.16	25.40
Non Islanding Condition 3	39.48	34.20	31.54	29.34	34.84	28.98
Non Islanding Condition 4	37.08	30.62	26.96	25.86	30.22	23.18

challenging nowadays. The islanding condition of distributed generation should be detected due to safety reasons and to maintain quality of power supplied to the customers. Voltage histogram based analysis is proposed for islanding detection of wind turbines in this paper. Reducing the NDZ to as close as possible and fast detection of it are the main contributions of the proposed technique in this paper. In order to show the performance of the proposed method, the test wind turbine system was simulated in MATLAB software. Six islanding conditions in NDZ and four switching conditions in test system were simulated, and the proposed islanding detection was applied to these conditions.

The results show the suitable reliability of the proposed method under different load conditions, such as load and capacitor bank switching and motor starting that islanding detection under these conditions is difficult. The method was able to detect the islanding condition of an induction generator type of a wind turbine within less than 0.15 s.

REFERENCES

Cheng-Tao H, Jeu-Min L, Shyh-Jier H (2008). Enhancement of islanding-detection of distributed generation systems via wavelet transform-based approaches. Int. J. Electri. Power Energy Syst., Vol. 30:10, pp 575-580.

Chowdhury SP, Chowdhury S, Crossley PA (2009). Islanding protection of activedistribution networks with renewable distributed generators: a comprehensivesurvey. Electr. Power Syst. Res.t. Res., December, 1-9.

Dash PK, Malhar P, Barik SK (2012). 'Estimation of power quality indices in distributed generation systems during power islanding conditions' Int. J. Electri. Power Energy Syst., Vol. 36:1, p 18-30

El-Arroudi K, Joós G, Kamwa I, McGillis DT (2007). Intelligent based approach to islanding detection in distributed generation. IEEE Trans. on Power Deliv., 22(2): 825-35.

Hernández-González G, Iravani R (2006). Current injection for active islanding detection of Electronically-Interfaced distributed resources. IEEE Trans. On Power Deliv., 21(3): 1698-705.

http://www.renewableenergyworld.com/rea/news/article/2011/05/worldwind-outlook-down-but-not-out.

Jayaweera D, Galloway S, Burt G, McDonald JR (2007). A sampling approach for intentional islanding of distributed eneration. IEEE Trans. on Power Syst., 22(2): 514-21.

Jiayi H, Chuanwen J, Rong X (2008). A review on distributed energy resources and micro-grid. Renew, Sust. Energ Rev., 12: 2472-83.

John V, Ye Z, Kolwalkar A (2004). Investigation of anti islanding protection of power converter based distributed generators using frequency domain analysis. Trans. on Power Electronic, 19(5): 1177-83.

Karegar HK, Sobhani B (2012)., Wavelet transform method for islanding detection of wind turbines, Renewable Energy 38:94-106

Karimi H, Yazdani A, Iravani R (2008). Negative-sequence current injection for fast islanding detection of distributed resource unit. IEEE Trans. on Power Deliv., 23(1): 493-501.

Kunte SR, Gao W (2008). Comparison and review of islanding detection techniques for distributed energy resources. IEEE, Conference; 1-8.

Swisher R, De Azua CR, Clendenin J (2001). Strong winds on the horizon: wind power comes of age. Proceedings of the IEEE, 89(12): 1757-64.

Wen-Jung C, Hurng-Liahng J, Jinn-Chang W (2012). 'Active islanding detection method for inverter-based distribution generation power' Int. J. Electri. Power Energy Syst., Vol. 42:1, pp 158-166

Xu W, Mauch K, Martel S (2004). An assessment of DG islanding detection methods and issues for Canada. CETC-Varennes 2004-074 (TR) 411-INVERT. 1-6.

Zeineldin HH, Abdel-Galil T, El-Saadany EF, Salama MMA (2007). Islanding detection of grid connected distributed generators using TLS-ESPRIT. Electr. Power Syst. Res., 77: 155-62.

Zeineldin HH, EL-Saadany EF, Salama MMA (2006). 'Islanding Detection of Inverter Based distributed Generation'. IEE Proc.Gener.Transm.Distrib.- Nov 2006, Vol. 153:6, pp.644-652

Zeineldin HH, El-Saadany Ehab F, Salama MMA (2006). Impact of DG interface control on islanding detection and non-detection zones. IEEE Trans Power Delivery, 21(3):1515–23.

Zhihong Y, Kolwalkar A, Zhang Y, Du P, Walling R(2004). Evaluation of anti-islanding schemes based on non detection zone concept. IEEE Trans. of Power Electronic. 19: 1171-6.